

# Approximate analytical description for the nonlinear $\mathcal{PT}$ -symmetric coupled-mode equations

Bowen Li<sup>1</sup>, Tao Xu<sup>1</sup> , Jianjun Liu<sup>1</sup> and Min Li<sup>2</sup>

<sup>1</sup> College of Science, China University of Petroleum, Beijing 102249, People's Republic of China

<sup>2</sup> School of Mathematics and Physics, North China Electric Power University, Beijing 102206, People's Republic of China

E-mail: [xutao@cup.edu.cn](mailto:xutao@cup.edu.cn)

Received 8 September 2019, revised 30 October 2019

Accepted for publication 20 November 2019

Published 10 February 2020



CrossMark

## Abstract

In this paper, we present an approximate analytical description of the solutions dynamics of nonlinear  $\mathcal{PT}$ -symmetric coupled-mode equations which can be used to realize the nonlinear  $\mathcal{PT}$ -symmetric optical configuration. By the multiple-scale analysis, we construct the asymptotic solutions of the coupled-mode equations. In the  $\mathcal{PT}$ -symmetry unbroken region, there is a good agreement between the asymptotic solutions and exact numerical solutions, and the higher-order asymptotic series can yield a higher accuracy. However, in the  $\mathcal{PT}$ -symmetry broken region, the asymptotic solutions become invalid quickly as  $z$  increases. Instead, we neglect one linear coupling term and obtain the approximate analytical solutions which, to some extent, describe the dynamics in the  $\mathcal{PT}$ -symmetry broken region when  $z \gg 1$ . This paper may be helpful for undergraduate and graduate students in physics to understand the nonlinear dynamics of  $\mathcal{PT}$ -symmetric systems.

Keywords:  $\mathcal{PT}$ -symmetric coupled-mode equations, asymptotic solutions,  $\mathcal{PT}$ -symmetry breaking, multiple-scale analysis

(Some figures may appear in colour only in the online journal)

## 1. Introduction

In quantum mechanics, the normalized linear Schrödinger equation ( $\hbar = m = 1$ ) is written as  $i\psi_t = H\psi$  with the Hamiltonian  $H = -\frac{1}{2}\frac{\partial^2}{\partial x^2} + V(x)$ , where  $V(x)$  is the static potential. Traditionally, it was believed that the Hamiltonian with a real-valued potential  $V(x)$  must be

Hermitian (i.e.,  $H = H^\dagger$ ) in order to ensure the measurement of real eigenenergy and unitary time evolution [1]. However, in 1998 Bender and Boettcher discovered that a wide class of complex non-Hermitian Hamiltonians can still show entirely real spectra provided that the Hamiltonian  $H$  respects the parity-time ( $\mathcal{PT}$ ) symmetry, that is,  $H$  commutes with the combined parity operator ( $\mathcal{P}$ ) and time-reversal operator ( $\mathcal{T}$ ) [2]. Here, the operators  $\mathcal{P}$  and  $\mathcal{T}$  are defined by [1]

$$\begin{aligned}\mathcal{P}: \quad \hat{x} &\rightarrow -\hat{x}, \quad \hat{p} \rightarrow -\hat{p}, \\ \mathcal{T}: \quad \hat{x} &\rightarrow \hat{x}, \quad \hat{p} \rightarrow -\hat{p}, \quad i \rightarrow -i,\end{aligned}\tag{1}$$

where  $\hat{p}$  and  $\hat{x}$  are the momentum and position operators, respectively. The communication relation between  $H$  and  $\mathcal{PT}$  suggests that a necessary condition for a non-Hermitian Hamiltonian to be  $\mathcal{PT}$  symmetric is  $V(x) = V^*(-x)$ , which implies that the real part of  $V(x)$  must be an even function while the imaginary part should be an odd one. But unlike the Hermiticity, the requirement of  $\mathcal{PT}$  symmetry is not sufficient for  $H$  to possess the entirely real spectrum. In fact, the  $\mathcal{PT}$ -symmetric Hamiltonians admit two parametric regions [2–6]: (i) In the  $\mathcal{PT}$ -symmetry unbroken region, every eigenfunction of  $H$  is also an eigenfunction of the  $\mathcal{PT}$  operator and all the eigenvalues are real; (ii) In the  $\mathcal{PT}$ -symmetry broken region, some of the eigenfunctions of  $H$  are not simultaneously the eigenfunctions of the  $\mathcal{PT}$  operator and there are a finite number of real and infinite number of complex conjugate pairs of eigenvalues. Therefore,  $\mathcal{PT}$ -symmetric systems often exhibit a spontaneous  $\mathcal{PT}$  symmetry-breaking (namely, a phase transition from the unbroken to broken  $\mathcal{PT}$  phase) when the non-Hermiticity parameter exceeds a certain critical value.

Since the pioneering work of Bender and Boettcher [2], many efforts have been made to extend the framework of quantum theory into the complex domain by revisiting the standard axiom of Hermiticity [3–8]. Meanwhile, the concept of  $\mathcal{PT}$  symmetry has also spread to optics [9, 10], classical mechanics [11], complex crystals [12], quantum chromodynamics [13], electronic circuits [14], mathematical physics [15, 16] and so on. Especially, optics provides a fertile ground for testing and realizing the  $\mathcal{PT}$ -related concepts [9, 10] owing to the mathematical similarity between the Schrödinger equation in quantum mechanics and the paraxial equation of diffraction in optics [17–19]. In fact, given that the complex refractive-index distribution  $n(x) = n_R(x) + in_I(x)$  (where  $n_R(x)$  is the refractive index profile while  $n_I(x)$  represents the gain/loss distribution) plays the role of an optical potential, one can design a  $\mathcal{PT}$ -symmetric system by requiring  $n_R(x) = n_R(-x)$  and  $n_I(x) = -n_I(-x)$  [9, 10, 17–19]. Over the past decade, the  $\mathcal{PT}$ -symmetry breaking within the realm of optics was observed in experiment [9, 10], and the dynamics of linear and nonlinear  $\mathcal{PT}$ -symmetric systems was also studied extensively in theory (see review in [20, 21]).

The simplest  $\mathcal{PT}$ -symmetric optical configuration can be realized in a pair of coupled waveguides (i.e. optical coupler) with balanced gain and loss [9, 19]. Based on the coupled-mode approximation, the leading order of the paraxial diffraction equation can yield the linear  $\mathcal{PT}$ -symmetric coupled-mode equations [9, 19]

$$i\frac{dE_1(z)}{dz} - i\frac{\gamma}{2}E_1(z) + \kappa E_2(z) = 0,\tag{2a}$$

$$i\frac{dE_2(z)}{dz} + i\frac{\gamma}{2}E_2(z) + \kappa E_1(z) = 0,\tag{2b}$$

which are referred to as the linear  $\mathcal{PT}$ -symmetric coupler, where  $z$  is the propagation distance,  $E_{1,2}(z)$  are the mode amplitudes in the two waveguides,  $\gamma$  represents the rate of gain in the first waveguide and loss in the second waveguide,  $\kappa$  is the coupling coefficient. System (2) is

exactly solvable and undergoes the phase transition from unbroken to broken  $\mathcal{PT}$  symmetry at the point  $\gamma = 2\kappa$  [9, 10].

With the inclusion of the Kerr nonlinearity, one can also derive the nonlinear  $\mathcal{PT}$ -symmetric coupled-mode equations [22, 23]:

$$i \frac{dE_1(z)}{dz} - i \frac{\gamma}{2} E_1(z) + \kappa E_2(z) + \epsilon |E_1|^2 E_1 = 0, \quad (3a)$$

$$i \frac{dE_2(z)}{dz} + i \frac{\gamma}{2} E_2(z) + \kappa E_1(z) + \epsilon |E_2|^2 E_2 = 0, \quad (3b)$$

which are usually called the nonlinear  $\mathcal{PT}$ -symmetric coupler [20], where  $|E_1|^2 E_1$  and  $|E_2|^2 E_2$  represent the Kerr nonlinearities, and  $\epsilon$  characterizes the nonlinear strength. Such a nonlinear  $\mathcal{PT}$ -symmetric coupler has potential applications in all-optical signal manipulation with ultralow-power and high-contrast switching [24]. In mathematics, system (3) is fully integrable because of the existence of conserved quantities [25, 26]. Similarly to the linear case, there also exists a threshold of symmetry breaking in the nonlinear  $\mathcal{PT}$ -symmetric coupler. In fact, system (3) admits two classes of solutions [22, 23]: (i) periodic solutions with the intensities and relative phases in two waveguides being exactly restored after each period, and (ii) solutions with the intensity growing without bound due to the nonlinearity-induced symmetry breaking. However, in spite that the existence of such two classes of solutions has been identified [23, 26–28], it is very hard to derive them in the explicit form (except that some particular cases were obtained explicitly, e.g. as seen in [28]).

In this paper, we aim to construct the asymptotic solutions of the nonlinear  $\mathcal{PT}$ -symmetric coupler (3), and understand the nonlinear dynamics in both the  $\mathcal{PT}$ -symmetry broken and unbroken regions. We present this to undergraduate and graduate students majoring in physics. This exploration could be used as an assignment project for students when they are studying courses like Methods of Mathematical Physics. Prior knowledge mainly includes the ordinary differential equations and quantum mechanics. The structure of this paper is arranged as follows. In section 2, we review the exact analytical solutions of the linear  $\mathcal{PT}$ -symmetric coupler (2), and draw the phase portraits around the equilibrium point. In section 3, by employing the multiple-scale analysis, we obtain the asymptotic solutions of system (3) in both the  $\mathcal{PT}$ -symmetry unbroken and broken regions. By comparison, we find that the asymptotic solutions give a good agreement to the exact numerical solutions when  $\gamma < 2\kappa$ , but the asymptotic solutions become invalid quickly as  $z$  increases when  $\gamma > 2\kappa$ . Then, we derive the approximate analytical solutions of system (3) with  $\gamma > 2\kappa$  by neglecting one linear coupling term, so as to approximately describe the solution behavior when  $z \gg 1$ . In section 4, we address the conclusions of this paper.

## 2. Exact analytical solutions and phase portraits of linear $\mathcal{PT}$ -symmetric coupled-mode equations

First, we give a short review of the exact analytical solutions of system (2), which were earlier obtained in [4, 5, 9, 10]. For convenience, we write system (2) in the matrix form

$$i \frac{d}{dz} \begin{pmatrix} E_1 \\ E_2 \end{pmatrix} = H \begin{pmatrix} E_1 \\ E_2 \end{pmatrix}, \quad H = \begin{pmatrix} i \frac{\gamma}{2} & -\kappa \\ -\kappa & -i \frac{\gamma}{2} \end{pmatrix}, \quad (4)$$

where  $H$  is the  $2 \times 2$  Hamiltonian matrix. The eigenvalues  $\beta$  and eigenvectors  $\vec{\phi}$  for system (4) can be obtained as follows:

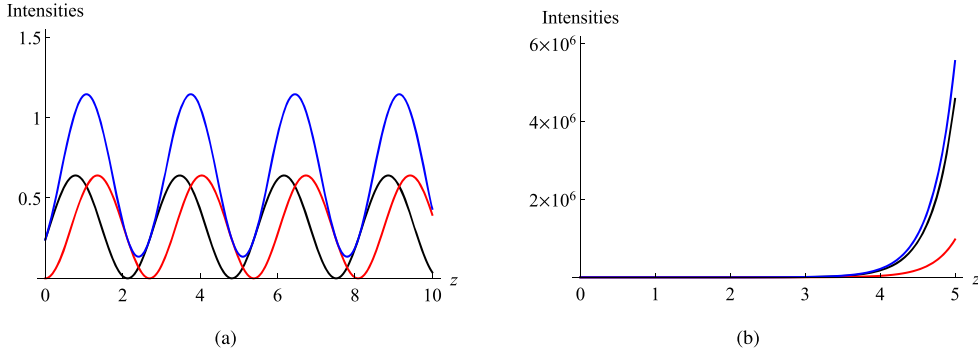


**Figure 1.** (a) Evolution of periodic solutions for system (4) with  $\kappa = 1.9$  and  $\gamma = 3$ . (b) Evolution of exponentially-growing solutions for system (4) with  $\kappa = 1.9$  and  $\gamma = 5$ . The black and red solid lines are respectively plotted for the fields  $E_1$  and  $E_2$ , whereas the blue solid line represents the total intensity of two fields.

$$\beta_{1,2} = \begin{cases} \pm \sqrt{\kappa^2 - \frac{\gamma^2}{4}} & \gamma < 2\kappa, \\ 0 & \gamma = 2\kappa, \\ \pm i \sqrt{\frac{\gamma^2}{4} - \kappa^2} & \gamma > 2\kappa, \end{cases} \quad (5)$$

and

$$\vec{\phi}_{1,2} = \begin{cases} \left(1, \pm \frac{-1}{e^{\pm i\omega}}\right)^T & \gamma < 2\kappa, \\ (1, i)^T & \gamma = 2\kappa, \\ \left(1, \frac{i}{e^{\pm i\omega}}\right)^T & \gamma > 2\kappa, \end{cases} \quad (6)$$

where the subscripts ‘1’ and ‘2’ respectively correspond to the signs ‘+’ and ‘-’,  $T$  denotes the vector transpose, and  $\omega$  is defined by

$$\omega = \begin{cases} \arcsin\left(\frac{\gamma}{2\kappa}\right) & \gamma < 2\kappa, \\ \operatorname{arccosh}\left(\frac{\gamma}{2\kappa}\right) & \gamma > 2\kappa. \end{cases} \quad (7)$$

It can be seen from equations (5) and (6) that the spectrum associated to system (4) is either purely real or imaginary, depending on the ratio of  $\gamma$  and  $\kappa$ . When  $\gamma < 2\kappa$ , the  $\mathcal{PT}$ -symmetry is unbroken (both eigenvalues are real), the eigenfunctions are both periodically bounded for all  $z \in \mathbb{R}^+$  and the total intensity in two fields is also periodically oscillating (see figure 1(a)). For  $\gamma > 2\kappa$ , the  $\mathcal{PT}$ -symmetry is broken (both eigenvalues are imaginary), the eigenfunctions and the total intensity grow exponentially to  $\infty$  as  $z \rightarrow \infty$  (see figure 1(b)). At  $\gamma = 2\kappa$ , the two eigenvalues collide and the eigenvectors become linearly dependent. Thus, the  $\mathcal{PT}$ -symmetry breaking occurs at this point, which is called an exceptional point or branch point [29].

Meanwhile, the general solutions of system (4) with  $\gamma \neq 2\kappa$  can be given by

$$\begin{pmatrix} E_1 \\ E_2 \end{pmatrix} = C_1 \exp(-i\beta_1 z) \vec{\phi}_1 + C_2 \exp(-i\beta_2 z) \vec{\phi}_2, \quad (8)$$

where  $C_1$  and  $C_2$  are arbitrary constants in  $\mathbb{C}$ . Equivalently, the general solutions can be written as

$$E_1(z) = C_1 E_1^{(1)} + C_2 E_1^{(2)}, \quad E_2(z) = C_1 E_2^{(1)} + C_2 E_2^{(2)}, \quad (9)$$

with  $E_1^{(1,2)}$  and  $E_2^{(1,2)}$  given by

$$E_1^{(1)} = \begin{cases} \exp(-i\kappa z \cos \omega) & \gamma < 2\kappa, \\ \exp(\kappa z \sinh \omega) & \gamma > 2\kappa, \end{cases} \quad E_1^{(2)} = \begin{cases} \exp(i\kappa z \cos \omega) & \gamma < 2\kappa, \\ \exp(-\kappa z \sinh \omega) & \gamma > 2\kappa, \end{cases} \quad (10)$$

and

$$E_2^{(1)} = \begin{cases} -e^{-i\omega} \exp(-i\kappa z \cos \omega) & \gamma < 2\kappa, \\ ie^{-\omega} \exp(\kappa z \sinh \omega) & \gamma > 2\kappa, \end{cases} \quad E_2^{(2)} = \begin{cases} e^{i\omega} \exp(i\kappa z \cos \omega) & \gamma < 2\kappa, \\ ie^{\omega} \exp(-\kappa z \sinh \omega) & \gamma > 2\kappa, \end{cases} \quad (11)$$

where  $\omega$  has been defined in equation (7). Particularly for  $\gamma = 2\kappa$ , the general solutions of system (4) read

$$E_1 = (C_1 + iC_2)\kappa z + C_1, \quad E_2 = (iC_1 - C_2)\kappa z + C_2. \quad (12)$$

In the language of optics, the eigenvalues and eigenvectors of  $H$  respectively correspond to the propagation constants and supermodes in the  $\mathcal{PT}$ -symmetric coupled waveguides. For the  $\gamma < 2\kappa$  case which corresponds to the real propagation constants, the fields  $E_1$  and  $E_2$  have the same intensities but there exists a relative phase difference, as shown in figure 1(a). Meanwhile, their individual intensities as well as the total intensity exhibit the periodical power oscillation. When  $\gamma > 2\kappa$  associated with a pair of conjugate propagation constants, both the intensities of  $E_1$  and  $E_2$  in general display the exponential growth behavior at  $z > 0$  (the exponential decay occurs only when  $C_1 = 0$ ), as seen in figure 1(b). But the former grows faster than the latter with the factor  $e^{2\text{arccosh}(\frac{\gamma}{2\kappa})}$ , so that the supermodes are biased to the gain waveguide. In both the  $\mathcal{PT}$  symmetry unbroken and broken regions, the light propagation is non-reciprocal and this behavior is more obvious beyond the phase-transition point. This signature may be used to develop new optical components, e.g. the optical isolator [30]. Particularly at the branch point  $\gamma = 2\kappa$ , the two propagation constants collide and two supermodes coalesce to a single eigenstate, featuring the non-Hermitian degeneracy. From a practical point of view, the unidirectional invisibility can be achieved in some designed  $\mathcal{PT}$ -symmetric periodic structures near the spontaneous  $\mathcal{PT}$ -symmetry breaking point [31, 32].

Next, we draw the phase portraits around the equilibrium point  $(0, 0)$  so as to qualitatively understand the stability of the solutions of system (4). Note that the Hamiltonian  $H$  of system (4) is a complex matrix, so that the real and imaginary parts of  $E_1$  and  $E_2$  no longer solve the same system. Hence, we cannot directly draw the phase portrait in the  $(E_1, E_2)$ -plane, and cannot judge the type of the equilibrium point  $(0, 0)$  based on the eigenvalues of  $H$ , either. To overcome this difficulty, we transform system (4) equivalently to a system with the real coefficient matrix.

When  $\gamma < 2\kappa$ , via the transformation

$$\xi = -i\kappa E_1 + \frac{\gamma}{2} E_2, \quad \eta = \sqrt{\kappa^2 - \frac{\gamma^2}{4}} E_2, \quad (13)$$

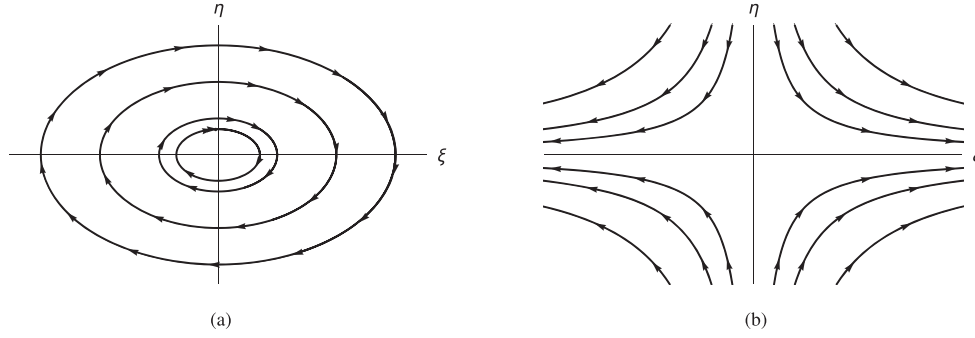


**Figure 2.** (a) Phase portrait around the centre  $(0, 0)$  for system (14) with  $\kappa = 1.9$  and  $\gamma = 3$ . (b) Phase portrait around the saddle  $(0, 0)$  for system (14) with  $\kappa = 1.9$  and  $\gamma = 5$ .

system (4) becomes

$$\begin{cases} \frac{d\xi}{dz} = \sqrt{\kappa^2 - \frac{\gamma^2}{4}} \eta, \\ \frac{d\eta}{dz} = -\sqrt{\kappa^2 - \frac{\gamma^2}{4}} \xi. \end{cases} \quad (14)$$

Then, it becomes feasible to draw the phase portrait for system (14) in the  $(\xi, \eta)$ -plane. Noticing that system (14) has two pure imaginary eigenvalues  $\pm i\sqrt{\kappa^2 - \frac{\gamma^2}{4}}$ , we know that the equilibrium point  $(0, 0)$  is a centre and the solutions are neutrally stable (see figure 2(a)). Therefore, we can say that  $(0, 0)$  is also a centre for system (4), which can be confirmed by observing that the solutions of system (4) are bounded and periodically oscillating, as shown in figure 1(a).

Similarly, when  $\gamma > 2\kappa$ , through the transformation

$$\xi = \left(-\frac{\gamma}{2} - \sqrt{\frac{\gamma^2}{4} - \kappa^2}\right)E_1 - i\kappa E_2, \quad \eta = \left(-\frac{\gamma}{2} + \sqrt{\frac{\gamma^2}{4} - \kappa^2}\right)E_1 - i\kappa E_2, \quad (15)$$

system (4) becomes

$$\begin{cases} \frac{d\xi}{dz} = \sqrt{\frac{\gamma^2}{4} - \kappa^2} \xi, \\ \frac{d\eta}{dz} = -\sqrt{\frac{\gamma^2}{4} - \kappa^2} \eta. \end{cases} \quad (16)$$

Here, system (16) has two real eigenvalues in which one is negative and the other is positive. Accordingly, the equilibrium point  $(0, 0)$  is a saddle of system (4) (see figure 2(b)) and the solutions are unstable, which can be confirmed from the solutions exhibiting the exponential growth behavior as displayed in figure 1(b).

### 3. Approximate analytical solutions of nonlinear $\mathcal{PT}$ -symmetric coupled-mode equations

In this section, we construct the approximate analytical solutions of the nonlinear  $\mathcal{PT}$ -symmetric coupler (3). As we know, the multiple-scale analysis is very effective in obtaining a uniformly valid approximation to the solutions of perturbation problems [33].

Generally, this can be done by introducing the time- or spatial-scale variables and regarding them to be independent of one another. Meanwhile, the original ordinary differential equations need be treated as partial differential equations.

To begin with, we regard the nonlinearity coefficient  $\epsilon$  in system (3) as a small parameter, and introduce a new variable  $\tau = \epsilon z$ , where  $\tau$  defines a long spatial scale since it is not negligible when  $z$  is of the order  $1/\epsilon$  or larger. Then, we expand the solutions of system (3) in the following form:

$$E_1(z) = E_{1,0}(z, \tau) + \epsilon E_{1,1}(z, \tau) + O(\epsilon^2), \quad (17a)$$

$$E_2(z) = E_{2,0}(z, \tau) + \epsilon E_{2,1}(z, \tau) + O(\epsilon^2). \quad (17b)$$

Via the chain rule, we compute the derivatives of  $E_{1,2}(z)$ :

$$\frac{dE_1}{dz} = \frac{\partial E_{1,0}}{\partial z} + \epsilon \left( \frac{\partial E_{1,0}}{\partial \tau} + \frac{\partial E_{1,1}}{\partial z} \right) + O(\epsilon^2), \quad (18a)$$

$$\frac{dE_2}{dz} = \frac{\partial E_{2,0}}{\partial z} + \epsilon \left( \frac{\partial E_{2,0}}{\partial \tau} + \frac{\partial E_{2,1}}{\partial z} \right) + O(\epsilon^2). \quad (18b)$$

Substituting equations (17) and (18) into system (3) and collecting the coefficients for the same powers of  $\epsilon$  gives

$$\epsilon^0: \quad i \frac{\partial E_{1,0}}{\partial z} = i \frac{\gamma}{2} E_{1,0} - \kappa E_{2,0}, \quad (19a)$$

$$\epsilon^0: \quad i \frac{\partial E_{2,0}}{\partial z} = -i \frac{\gamma}{2} E_{2,0} - \kappa E_{1,0}, \quad (19b)$$

$$\epsilon^1: \quad i \frac{\partial E_{1,1}}{\partial z} - i \frac{\gamma}{2} E_{1,1} + \kappa E_{2,1} = -i \frac{\partial E_{1,0}}{\partial \tau} - |E_{1,0}|^2 E_{1,0}, \quad (19c)$$

$$\epsilon^1: \quad i \frac{\partial E_{2,1}}{\partial z} + i \frac{\gamma}{2} E_{2,1} + \kappa E_{1,1} = -i \frac{\partial E_{2,0}}{\partial \tau} - |E_{2,0}|^2 E_{2,0}. \quad (19d)$$

In what follows, we solve the above equations in the  $\mathcal{PT}$ -symmetry unbroken ( $\gamma < 2\kappa$ ) and broken ( $\gamma > 2\kappa$ ) regions, respectively.

### 3.1. Case I: $\gamma < 2\kappa$

Since equations (19a) and (19b) have the same form as that of equations (2a) and (2b), we first obtain the general solutions for  $E_{1,0}$  and  $E_{2,0}$  as follows:

$$E_{1,0} = A(\tau) e^{i\kappa z \cos \omega} + B(\tau) e^{-i\kappa z \cos \omega}, \quad (20a)$$

$$E_{2,0} = A(\tau) e^{i(\omega + \kappa z \cos \omega)} - B(\tau) e^{-i(\omega + \kappa z \cos \omega)}, \quad (20b)$$

where  $\cos \omega = \sqrt{1 - \frac{\gamma^2}{4\kappa^2}}$ ,  $A(\tau)$  and  $B(\tau)$  are two complex-valued functions of  $\tau$ .

Then, plugging equations (20a) and (20b) into the right-hand sides of equations (19c) and (19d) yields

$$i\frac{\partial E_{1,1}}{\partial z} - i\frac{\gamma}{2}E_{1,1} + \kappa E_{2,1} = -\left(i\frac{dA}{d\tau} + |A|^2A + 2A|B|^2\right)e^{i\kappa z \cos \omega} - A^2B^*e^{3i\kappa z \cos \omega} - \left(i\frac{dB}{d\tau} + |B|^2B + 2|A|^2B\right)e^{-i\kappa z \cos \omega} - A^*B^2e^{-3i\kappa z \cos \omega}, \quad (21a)$$

$$i\frac{\partial E_{2,1}}{\partial z} + i\frac{\gamma}{2}E_{2,1} + \kappa E_{1,1} = -\left(i\frac{dA}{d\tau} + |A|^2A + 2A|B|^2\right)e^{i(\omega+\kappa z \cos \omega)} + A^2B^*e^{3i(\omega+\kappa z \cos \omega)} - \left(i\frac{dB}{d\tau} + |B|^2B + 2|A|^2B\right)e^{-i(\omega+\kappa z \cos \omega)} - A^*B^2e^{-3i(\omega+\kappa z \cos \omega)}, \quad (21b)$$

where the asterisk denotes complex conjugate. Note that  $(e^{i\kappa z \cos \omega}, e^{i(\omega+\kappa z \cos \omega)})^T$  and  $(e^{-i\kappa z \cos \omega}, -e^{-i(\omega+\kappa z \cos \omega)})^T$  are two elementary solutions of the homogeneous counterparts of equations (21a) and (21b). In order to avoid the appearance of the secular terms, we must require the functions  $A(\tau)$  and  $B(\tau)$  satisfy

$$i\frac{dA}{d\tau} + |A|^2A + 2A|B|^2 = 0, \quad (22a)$$

$$i\frac{dB}{d\tau} + |B|^2B + 2|A|^2B = 0. \quad (22b)$$

By writing  $A(\tau)$  and  $B(\tau)$  in the polar form  $A(\tau) = R_1(\tau)e^{i\theta_1(\tau)}$  and  $B(\tau) = R_2(\tau)e^{i\theta_2(\tau)}$  and substituting them into equations (22a) and (22b), we obtain that

$$i\frac{dR_1}{d\tau} - R_1\frac{d\theta_1}{d\tau} + R_1^3 + 2R_1R_2^2 = 0, \quad (23a)$$

$$i\frac{dR_2}{d\tau} - R_2\frac{d\theta_2}{d\tau} + R_2^3 + 2R_1^2R_2 = 0, \quad (23b)$$

where  $R_{1,2}(\tau)$  and  $\theta_{1,2}(\tau)$  are the real-valued functions to be determined. The imaginary parts of equations (23a) and (23b) equating to zeros indicates that  $R_1 = R_{1,0}$ ,  $R_2 = R_{2,0}$  with  $R_{1,0}$  and  $R_{2,0}$  being two real constants, whereas the remaining real parts give the solutions for  $\theta_{1,2}$ :

$$\theta_1 = (R_{1,0}^2 + 2R_{2,0}^2)\tau + \theta_{1,0}, \quad \theta_2 = (R_{2,0}^2 + 2R_{1,0}^2)\tau + \theta_{2,0}, \quad (24)$$

where  $\theta_{1,0}$  and  $\theta_{2,0}$  are two real constants. Therefore, we arrive at the zeroth-order asymptotic solutions of system (3) with  $\gamma < 2\kappa$  as follows:

$$E_1 = R_{1,0} e^{i[\epsilon(R_{1,0}^2+2R_{2,0}^2)z+\theta_{1,0}]+i\kappa z \cos \omega} + R_{2,0} e^{i[\epsilon(R_{2,0}^2+2R_{1,0}^2)z+\theta_{2,0}]-i\kappa z \cos \omega} + O(\epsilon), \quad (25a)$$

$$E_2 = R_{1,0} e^{i[\epsilon z(R_{1,0}^2+2R_{2,0}^2)+\theta_{1,0}]+i(\omega+\kappa z \cos \omega)} - R_{2,0} e^{i[\epsilon z(R_{2,0}^2+2R_{1,0}^2)+\theta_{2,0}]-i(\omega+\kappa z \cos \omega)} + O(\epsilon). \quad (25b)$$

Continually, we construct the first-order asymptotic solutions of system (3). With the secular terms dropped, equations (21a) and (21b) can be written as

$$i\frac{\partial E_{1,1}}{\partial z} - i\frac{\gamma}{2}E_{1,1} + \kappa E_{2,1} = -A^2B^*e^{3i\kappa z \cos \omega} - A^*B^2e^{-3i\kappa z \cos \omega}, \quad (26a)$$

$$i\frac{\partial E_{2,1}}{\partial z} + i\frac{\gamma}{2}E_{2,1} + \kappa E_{1,1} = A^2B^*e^{3i\omega+3i\kappa z \cos \omega} - A^*B^2e^{-3i\omega-3i\kappa z \cos \omega}. \quad (26b)$$

By employing the Laplace transformation and assuming that  $X_{1,1}(s) = \mathcal{L}[E_{1,1}(z)]$ ,  $X_{2,1}(s) = \mathcal{L}[E_{2,1}(z)]$  equations (26a) and (26b) become



$$isX_{1,1}(s) - i\frac{\gamma}{2}X_{1,1}(s) + \kappa X_{2,1}(s) = -\frac{A^2 B^*}{s - 3i\kappa \cos \omega} - \frac{A^* B^2}{s + 3i\kappa \cos \omega}, \quad (27a)$$

$$isX_{2,1}(s) + i\frac{\gamma}{2}X_{2,1}(s) + \kappa X_{1,1}(s) = \frac{A^2 B^* e^{3i\omega}}{s - 3i\kappa \cos \omega} - \frac{A^* B^2 e^{-3i\omega}}{s + 3i\kappa \cos \omega}, \quad (27b)$$

which can be solved as

$$X_{1,1}(s) = \frac{1}{s^2 - \kappa^2 \cos^2 \omega} \left[ A^2 B^* \frac{\kappa e^{3i\omega} + i(s + \frac{\gamma}{2})}{s - 3i\kappa \cos \omega} - A^* B^2 \frac{\kappa e^{-3i\omega} - i(s + \frac{\gamma}{2})}{s + 3i\kappa \cos \omega} \right], \quad (28a)$$

$$X_{2,1}(s) = \frac{1}{s^2 - \kappa^2 \cos^2 \omega} \left[ -A^2 B^* \frac{\kappa + i(s - \frac{\gamma}{2})e^{3i\omega}}{s - 3i\kappa \cos \omega} - A^* B^2 \frac{\kappa - i(s - \frac{\gamma}{2})e^{-3i\omega}}{s + 3i\kappa \cos \omega} \right]. \quad (28b)$$

Then, taking the inverse Laplace transformations for  $X_{1,1}$  and  $X_{2,1}$ , we have

$$E_{1,1} = \frac{(1+i)J^{-1}e^{-(1+3i)Kz}}{40K^2} \left\{ A^* B^2 [(1+2i)(2\kappa - i\gamma J - 2iJK)e^{(2+3i)Kz} \right. \\ - (1-i)(i\gamma J + 6JK - 2\kappa)e^{Kz} + (1-2i)(2JK - \gamma J - 2i\kappa)e^{3iKz}] \\ + A^2 B^* J [(2+i)(i\gamma + 2J\kappa + 2iK)e^{(2+3i)Kz} \\ \left. - (1-i)(2J\kappa + i\gamma - 6K)e^{(1+6i)Kz} - (1+2i)(2J\kappa + i\gamma - 2iK)e^{3iKz}] \right\}, \quad (29a)$$

$$E_{2,1} = \frac{(1+i)J^{-1}e^{-(1+3i)Kz}}{40K^2} \left\{ A^* B^2 [(1+2i)(i\gamma + 2J\kappa - 2iK)e^{(2+3i)Kz} \right. \\ + (1+i)(\gamma - 2iJ\kappa + 6iK)e^{Kz} - (2+i)(i\gamma + 2J\kappa + 2iK)e^{3iKz}] \\ + A^2 B^* J [(1+2i)(2\kappa - i\gamma J - 2iJK)e^{3iKz} \\ \left. + (2i-1)(\gamma J - 2JK + 2i\kappa)e^{(2+3i)Kz} - (1-i)(i\gamma J + 6JK - 2\kappa)e^{(1+6i)Kz}] \right\}, \quad (29b)$$

where  $J = e^{3i\omega}$  and  $K = \kappa \cos \omega$ . Hence, we arrive at the first-order asymptotic solutions of system (3) with  $\gamma < 2\kappa$  as follows:

$$E_1 = E_{1,0} + \epsilon E_{1,1} + O(\epsilon^2), \quad (30a)$$

$$E_2 = E_{2,0} + \epsilon E_{2,1} + O(\epsilon^2), \quad (30b)$$

where  $E_{1,0}$ ,  $E_{2,0}$ ,  $E_{1,1}$  and  $E_{2,1}$  are given by equations (25a), (25b), (29a) and (29b).

In figures 3(a) and (b), we plot the zeroth-order and first-order asymptotic solutions (25) and (30), and compare them with the exact numerical solutions. It can be clearly seen that there is a good agreement between the asymptotic solutions and exact numerical solutions. Meanwhile, we calculate the absolute errors between the asymptotic solutions and exact numerical solutions, as shown in figures 4(a) and (b). One can find that the errors for solutions (30) are much smaller than those for solutions (25), which implies that the high-order asymptotic expansion in (17) can yield a higher accuracy for system (3) in the  $\mathcal{PT}$ -symmetry unbroken region ( $\gamma < 2\kappa$ ). In addition, we note that the nonlinear  $\mathcal{PT}$ -symmetric coupler (3) with  $\gamma < 2\kappa$  also exhibits the periodical oscillation behavior of the total intensity, but there is a change for the oscillating frequency.

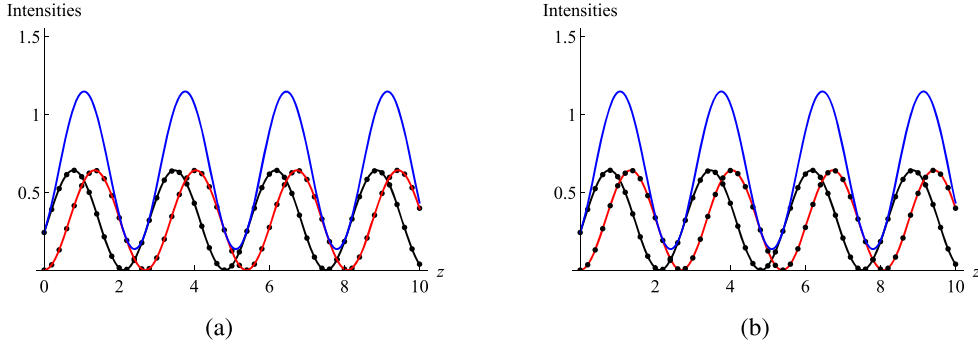


**Figure 3.** (a) Comparison between the exact numerical solutions (black dotted) and the zeroth-order asymptotic solutions (25) with  $R_{1,0} = 0.4$ ,  $R_{2,0} = 0.4$ ,  $\theta_{1,0} = -\omega$ ,  $\theta_{2,0} = \omega$ ,  $\kappa = 1.9$ ,  $\gamma = 3$ ,  $\epsilon = 0.1$ . (b) Comparison between the exact numerical solutions (black dotted) and the first-order asymptotic solutions (30) with the same values of parameters. The black and red solid lines are respectively plotted for the fields  $E_1$  and  $E_2$ , whereas the blue solid line represents the total intensity of two fields.

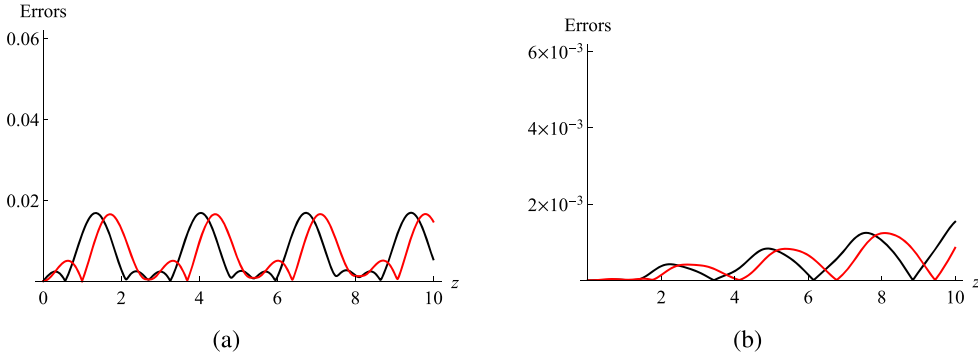


**Figure 4.** (a) Absolute errors between the zeroth-order asymptotic solutions (25) and exact numerical solutions. (b) Absolute errors between the first-order asymptotic solutions (30) and exact numerical solutions. The black and red solid lines are respectively associated to the fields  $E_1$  and  $E_2$ , and the parameters for asymptotic solutions are chosen the same as those in figures 3(a) and (b).

### 3.2. Case II: $\gamma > 2\kappa$

Similarly, we try to use the multiple-scale analysis to construct the asymptotic solutions of system (3) with  $\gamma > 2\kappa$ . In this case, the general solutions to equations (19a) and (19b) can be given as follows:

$$E_{1,0} = A(\tau)e^{\kappa z \sinh \omega} + B(\tau)e^{-\kappa z \sinh \omega}, \quad (31a)$$

$$E_{2,0} = iA(\tau)e^{-\omega + \kappa z \sinh \omega} + iB(\tau)e^{\omega - \kappa z \sinh \omega}, \quad (31b)$$

where  $\sinh \omega = \sqrt{\frac{\gamma^2}{4\kappa^2} - 1}$ ,  $A(\tau)$  and  $B(\tau)$  are two complex-valued functions of  $\tau$ . Substituting equations (31a) and (31b) into the right-hand sides of equations (19c) and (19d) yields

$$i\frac{\partial E_{1,1}}{\partial z} - i\frac{\gamma}{2}E_{1,1} + \kappa E_{2,1} = -\left(i\frac{dA}{d\tau} + 2|A|^2B + A^2B^*\right)e^{\kappa z \sinh \omega} - |A|^2Ae^{3\kappa z \sinh \omega} - \left(i\frac{dB}{d\tau} + 2A|B|^2 + A^*B^2\right)e^{-\kappa z \sinh \omega} - |B|^2Be^{-3\kappa z \sinh \omega}, \quad (32a)$$

$$i\frac{\partial E_{2,1}}{\partial z} + i\frac{\gamma}{2}E_{2,1} + \kappa E_{1,1} = -\left(i\frac{dA}{d\tau} + 2|A|^2B + A^2B^*\right)ie^{-\omega + \kappa z \sinh \omega} - i|A|^2Ae^{-3\omega + 3\kappa z \sinh \omega} - \left(i\frac{dB}{d\tau} + 2A|B|^2 + A^*B^2\right)ie^{\omega - \kappa z \sinh \omega} - i|B|^2Be^{3\omega - 3\kappa z \sinh \omega}. \quad (32b)$$

To eliminate the secular terms in the right-hands of equations (32a) and (32b), the functions  $A(\tau)$  and  $B(\tau)$  should satisfy

$$i\frac{dA}{d\tau} + 2|A|^2B + A^2B^* = 0, \quad (33a)$$

$$i\frac{dB}{d\tau} + 2A|B|^2 + A^*B^2 = 0. \quad (33b)$$

We write  $A(\tau) = R_1(\tau)e^{i\theta_1(\tau)}$  and  $B(\tau) = R_2(\tau)e^{i\theta_2(\tau)}$  ( $R_{1,2}$  and  $\theta_{1,2}$  are all the real-valued functions of  $\tau$ ) and substitute them into equations (33a) and (33b), giving

$$i\frac{dR_1}{d\tau} - R_1\frac{d\theta_1}{d\tau} + 2R_1^2R_2e^{i(\theta_2-\theta_1)} + R_1^2R_2e^{i(\theta_1-\theta_2)} = 0, \quad (34a)$$

$$i\frac{dR_2}{d\tau} - R_2\frac{d\theta_2}{d\tau} + 2R_1R_2^2e^{i(\theta_1-\theta_2)} + R_1R_2^2e^{i(\theta_2-\theta_1)} = 0, \quad (34b)$$

which, by separating the real and imaginary parts, give rise to

$$\frac{dR_1}{d\tau} = -R_1^2R_2\sin(\theta_2 - \theta_1), \quad (35a)$$

$$\frac{d\theta_1}{d\tau} = 3R_1R_2\cos(\theta_2 - \theta_1), \quad (35b)$$

$$\frac{dR_2}{d\tau} = R_1R_2^2\sin(\theta_2 - \theta_1), \quad (35c)$$

$$\frac{d\theta_2}{d\tau} = 3R_1R_2\cos(\theta_2 - \theta_1). \quad (35d)$$

By observation, one can find the following relations among  $\theta_1$ ,  $\theta_2$ ,  $R_1$  and  $R_2$ :

$$\frac{d(\theta_2 - \theta_1)}{d\tau} = 0, \quad R_2\frac{dR_1}{d\tau} + R_1\frac{dR_2}{d\tau} = 0. \quad (36)$$

Combining equations (35) with (36), we get the solutions:

$$R_1 = R_{2,0}e^{-R_{1,0}\sin(\theta_{1,0})\tau}, \quad R_2 = \frac{R_{1,0}}{R_{2,0}}e^{R_{1,0}\sin(\theta_{1,0})\tau}, \quad (37a)$$

$$\theta_1 = 3R_{1,0}\cos(\theta_{1,0})\tau + \theta_{2,0}, \quad \theta_2 = 3R_{1,0}\cos(\theta_{1,0})\tau + \theta_{1,0} + \theta_{2,0}, \quad (37b)$$

where  $\theta_{1,0}$ ,  $\theta_{2,0}$ ,  $R_{1,0}$ ,  $R_{2,0}$  are four real constants.

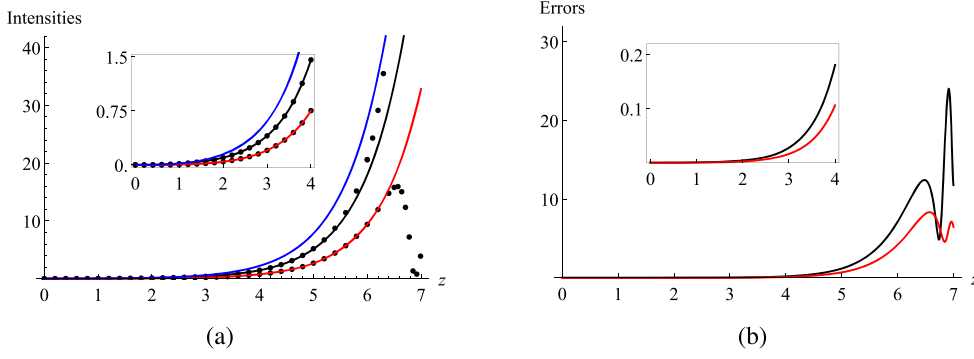


**Figure 5.** (a) Comparison between the exact numerical solutions (black dotted) and the zeroth-order asymptotic solutions (38) with  $R_{1,0} = -0.01$ ,  $R_{2,0} = 0.1$ ,  $\theta_{1,0} = 0$ ,  $\theta_{2,0} = 0$ ,  $\kappa = 1.9$ ,  $\gamma = 4$ ,  $\epsilon = 0.1$ . (b) Absolute errors between the asymptotic solutions (38) and exact numerical solutions. The black and red solid lines are respectively plotted for the fields  $E_1$  and  $E_2$ , whereas the blue solid line represents the total intensity of two fields.

Collecting all the above results, we obtain the zeroth-order asymptotic solutions of system (3) with  $\gamma > 2\kappa$  as follows:

$$E_1 = R_{2,0} e^{i[3\epsilon R_{1,0} \cos(\theta_{1,0})z + \theta_{2,0}] - \epsilon R_{1,0} \sin(\theta_{1,0})z + \kappa z \sinh \omega} + \frac{R_{1,0}}{R_{2,0}} e^{i[3\epsilon R_{1,0} \cos(\theta_{1,0})z + \theta_{1,0} + \theta_{2,0}] + \epsilon R_{1,0} \sin(\theta_{1,0})z - \kappa z \sinh \omega} + O(\epsilon), \quad (38a)$$

$$E_2 = iR_{2,0} e^{i[3\epsilon R_{1,0} \cos(\theta_{1,0})z + \theta_{2,0}] - \epsilon R_{1,0} \sin(\theta_{1,0})z + \kappa z \sinh \omega - \omega} + i \frac{R_{1,0}}{R_{2,0}} e^{i[3\epsilon R_{1,0} \cos(\theta_{1,0})z + \theta_{1,0} + \theta_{2,0}] + \epsilon R_{1,0} \sin(\theta_{1,0})z - \kappa z \sinh \omega + \omega} + O(\epsilon). \quad (38b)$$

To check the validity of asymptotic solutions (38), we compare them with the exact numerical solutions and calculate the absolute errors, as shown in figures 5(a) and (b). We find that the absolute errors in both the fields  $E_1$  and  $E_2$  go beyond the order  $10^{-1}$  when  $z > 4$ , which implies that the validity of asymptotic solutions (38) gets lost quickly with the increase of  $z$ . In fact, the exact numerical solutions show that  $|E_1|^2$  always displays an exponential growth without bound as  $z$  increases, whereas  $|E_2|^2$  grows at the initial stage and then decreases periodically when  $z > z_0$ . It is the unidirectional propagation characteristic that system (3) exhibits in the  $\mathcal{PT}$ -symmetry broken region [22, 23]. Therefore, since the term  $\epsilon |E_1|^2 E_1$  becomes much greater than the other terms in system (3) when  $z \gg 1$ , we cannot regard it as a small term in a comparable large range of  $z$ .

Next, we look for the approximate analytical solutions of system (3) with  $\gamma > 2\kappa$  when  $z \gg 1$ . Since the intensity of  $E_2$  becomes much smaller comparable to that of  $E_1$ , thus we neglect the term  $\kappa E_2(z)$  in equation (3a). Meanwhile, we replace  $\epsilon$  in equations (3a) and (3b) respectively with  $\epsilon_1$  and  $\epsilon_2$ , where  $\epsilon_1$  is regarded as a constant (because  $\epsilon_1 |E_1|^2 E_1$  is no longer a small term) but  $\epsilon_2$  still as a small parameter. Then, we solve the approximate equations to system (3) when  $z \gg 1$ :

$$i \frac{dE_1(z)}{dz} - i \frac{\gamma}{2} E_1(z) + \epsilon_1 |E_1|^2 E_1 = 0, \quad (39a)$$

$$i \frac{dE_2(z)}{dz} + i \frac{\gamma}{2} E_2(z) + \kappa E_1(z) + \epsilon_2 |E_2|^2 E_2 = 0. \quad (39b)$$

By assuming that  $E_1(z) = S_1(z)e^{iS_2(z)}$  (where  $S_{1,2}(z)$  are two real-valued functions), equation (39a) becomes

$$iS_1'(z) - S_1(z)S_2'(z) = i \frac{\gamma}{2} S_1(z) - \epsilon_1 S_1^3(z). \quad (40)$$

Separating the real and imaginary parts of equation (40) yields

$$S_1(z) = C_1 e^{\frac{\gamma}{2}z}, \quad S_2(z) = \frac{\epsilon_1 C_1^2}{\gamma} e^{\gamma z} + C_2, \quad (41)$$

where  $C_{1,2}$  are two arbitrary real constants. Then, we obtain the approximate analytical solution for  $E_1$ :

$$E_1(z) = C_1 e^{\frac{\gamma}{2}z + i \left( \frac{\epsilon_1 C_1^2}{\gamma} e^{\gamma z} + C_2 \right)}. \quad (42)$$

Furthermore, substituting equation (42) into (39b), we have

$$i \frac{dE_2(z)}{dz} + i \frac{\gamma}{2} E_2(z) + \kappa C_1 e^{\frac{\gamma}{2}z + i \left( \frac{\epsilon_1 C_1^2}{\gamma} e^{\gamma z} + C_2 \right)} + \epsilon_2 |E_2|^2 E_2 = 0. \quad (43)$$

Again, by the multiple-scale analysis for equation (43), we expand  $E_2$  in the asymptotic series form

$$E_2(z) = E_{2,0}(z, \tau) + \epsilon_2 E_{2,1}(z, \tau) + O(\epsilon_2^2). \quad (44)$$

Inserting it into equation (43) and equating the terms with the same powers of  $\epsilon_2$ , we have

$$\epsilon_2^0: \quad i \frac{\partial E_{2,0}}{\partial z} + i \frac{\gamma}{2} E_{2,0} = -\kappa C_1 e^{\frac{\gamma}{2}z + i \left( \frac{\epsilon_1 C_1^2}{\gamma} e^{\gamma z} + C_2 \right)}, \quad (45a)$$

$$\epsilon_2^1: \quad i \frac{\partial E_{2,1}}{\partial z} + i \frac{\gamma}{2} E_{2,1} = -i \frac{\partial E_{2,0}}{\partial \tau} - |E_{2,0}|^2 E_{2,0}. \quad (45b)$$

For equation (45a), we immediately obtain its general solution as follows:

$$E_{2,0} = A(\tau) e^{-\frac{\gamma}{2}z} + \frac{\kappa}{\epsilon_1 C_1} e^{-\frac{\gamma}{2}z + i \left( \frac{\epsilon_1 C_1^2}{\gamma} e^{\gamma z} + C_2 \right)}, \quad (46)$$

where  $A(\tau)$  is a complex-valued function to be determined. Then, substitution of equation (46) into equation (45b) gives

$$\begin{aligned} i \frac{\partial E_{2,1}}{\partial z} + i \frac{\gamma}{2} E_{2,1} = & -i A'(\tau) e^{-\frac{\gamma}{2}z} - e^{-\frac{\gamma}{2}z} \left[ \frac{A^* \kappa^2}{\epsilon_1^2 C_1^2} e^{2i \left( \frac{\epsilon_1 C_1^2}{\gamma} e^{\gamma z} + C_2 \right)} + \frac{A^2 \kappa}{\epsilon_1 C_1} e^{-i \left( \frac{\epsilon_1 C_1^2}{\gamma} e^{\gamma z} + C_2 \right)} \right. \\ & \left. + \left( \frac{2|A|^2 \epsilon_1^2 C_1^2 \kappa + \kappa^3}{\epsilon_1^3 C_1^3} \right) e^{i \left( \frac{\epsilon_1 C_1^2}{\gamma} e^{\gamma z} + C_2 \right)} + \left( 2 \frac{A \kappa^2}{\epsilon_1^2 C_1^2} + |A|^2 A \right) \right]. \end{aligned} \quad (47)$$

To eliminate the secular term in the right-hand side of equation (47), we must let  $A'(\tau) = 0$ , i.e.  $A(\tau) = C_3$  with  $C_3$  being a constant in  $\mathbb{C}$ . Therefore, we obtain the zeroth-order asymptotic solution for  $E_2$  as follows:

$$E_2 = C_3 e^{-\frac{\gamma}{2}z} + \frac{\kappa}{\epsilon_1 C_1} e^{-\frac{\gamma}{2}z + i \left( \frac{\epsilon_1 C_1^2}{\gamma} e^{\gamma z} + C_2 \right)}. \quad (48)$$

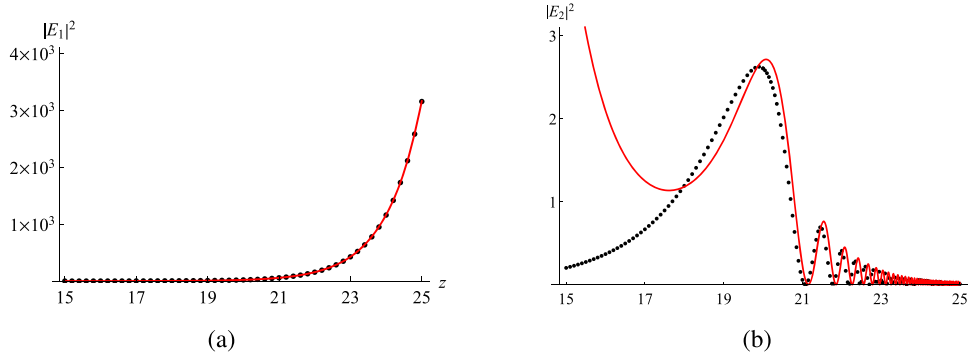


**Figure 6.** (a) Comparison between the exact numerical solution (black dotted) and approximate analytical solution (42) (red solid) for the field  $E_1$ , where  $C_1 = -0.002$ ,  $C_2 = -346758$ ,  $\kappa = 0.4$ ,  $\gamma = 1$ ,  $\epsilon_1 = \epsilon_2 = 0.1$ . (b) Comparison between the exact numerical solution (black dotted) and approximate analytical solution (48) (red solid) for the field  $E_2$ , where  $C_1 = -0.002$ ,  $C_2 = -346758$ ,  $C_3 = -6072 - 41043i$ ,  $\kappa = 0.4$ ,  $\gamma = 1$ ,  $\epsilon_1 = \epsilon_2 = 0.1$ .

Also, we compare the approximate analytical solutions (42) and (48) with the exact numerical solutions. In theory, the solutions of system (39) approach those of system (3) with  $\gamma > 2\kappa$  as  $z \rightarrow \infty$ . Thus, we match the approximate analytical solutions and numerical solutions at  $z = 32$  in figures 6(a) and (b). It can be found that the behaviors of solutions (42) and (48) are very similar to those of the exact numerical solutions when  $z \gg 1$ , that is,  $|E_1|^2$  grows exponentially without bound while  $|E_2|^2$  decays periodically to 0. However, some phase discrepancy still exists between the approximate analytical solutions and numerical solutions because the linear term  $\kappa E_2(z)$  is dropped.

#### 4. Conclusions

Recently, the  $\mathcal{PT}$ -symmetric systems have received intensive attention in quantum mechanics, optics and many other branches of physics. The simplest  $\mathcal{PT}$ -symmetric optical configuration with the Kerr nonlinearity can be modeled by the nonlinear  $\mathcal{PT}$ -symmetric coupled-mode equations (3a) and (3b). In this paper, we have given an approximate analytical description to the solutions dynamics of system (3). By using the multiple-scale analysis, we have constructed the asymptotic solutions in both the  $\mathcal{PT}$ -symmetry unbroken ( $\gamma < 2\kappa$ ) and broken ( $\gamma > 2\kappa$ ) regions. When  $\gamma < 2\kappa$ , there is a good agreement between the asymptotic solutions and exact numerical solutions, and the higher-order asymptotic series can yield a higher accuracy. However, for  $\gamma > 2\kappa$  the asymptotic solutions lose their validity quickly as  $z$  increases. Instead, by neglecting the term  $\kappa E_2(z)$  in system (3), we have obtained the approximate analytical solutions which, to some extent, describe the dynamics in the  $\mathcal{PT}$ -symmetry broken region when  $z \gg 1$ .

In fact, it is not difficult to expect the failure in constructing the asymptotic solutions of system (3) in the  $\mathcal{PT}$ -symmetry broken region. Note that the exact solutions (which are the same as solutions (9)) of the linear part of system (3) have a leading contribution in the asymptotic solutions (17), but their intensities with  $\gamma > 2\kappa$  grow exponentially to  $\infty$  as  $z$  increases. As a result,  $\epsilon |E_1|^2 E_1$  and  $\epsilon |E_2|^2 E_2$  become the dominant terms in system (3) when  $z$  exceeds a certain value. However, this violates that the nonlinear terms in system (3) should

be always regarded as small ones in the multiple-scale analysis, so that the asymptotic solutions (38) become invalid when  $z \gg 1$ .

Students can see that without solving the nonlinear system (3) exactly, one can still construct the approximate analytical solutions by some basic skills in ordinary differential equations. Based on the obtained solutions, they can acquire an understanding on the dynamics of nonlinear  $\mathcal{PT}$ -symmetric coupler. In addition, students can further study the solutions dynamics of nonlinear  $\mathcal{PT}$ -symmetric trimer [34] in a similar way.

## Acknowledgments

We would like to thank the anonymous referees for their valuable comments, and the helpful discussions with Professor Pengfei Li from Taiyuan Normal University. T X appreciates the hospitality of the Department of Mathematics & Statistics at McMaster University during his visit in 2019. This work was partially supported by the National Natural Science Foundation of China (Grant Nos. 11705284 and 61505054), by the Construction Program of Undergraduate Core Courses and the Quality and Innovation Project of Graduate Education from China University of Petroleum-Beijing, and by the program of China Scholarship Council (Grant No. 201806445009).

## ORCID iDs

Tao Xu  <https://orcid.org/0000-0002-2740-4780>

## References

- [1] Shankar R 1994 *Principles of Quantum Mechanics* (New York: Plenum Press)
- [2] Bender C M and Boettcher S 1998 *Phys. Rev. Lett.* **80** 5243
- [3] Bender C M, Brody D C and Jones H F 2002 *Phys. Rev. Lett.* **89** 270401
- [4] Bender C M 2007 *Rep. Prog. Phys.* **70** 947
- [5] Bender C M, Berry M and Mandilara A 2002 *J. Phys. A* **35** 467
- [6] Bender C M, Brody D C and Jones H F 2003 *Am. J. Phys.* **71** 1095
- [7] Berry M V 2004 *Czech J. Phys.* **54** 1039
- [8] Znojil M 2001 *Phys. Lett. A* **285** 7
- [9] Guo A, Salamo G J, Duchesne D, Morandotti R, Volatier-Ravat M, Aimez V, Siviloglou G A and Christodoulides D N 2009 *Phys. Rev. Lett.* **103** 093902
- [10] Rüter C E, Makris K G, El-Ganainy R, Christodoulides D N, Segev M and Kip D 2010 *Nat. Phys.* **6** 192
- [11] Bender C M, Berntson B K, Parker D and Samuel E 2013 *Am. J. Phys.* **81** 173
- [12] Longhi S 2009 *Phys. Rev. Lett.* **103** 123601
- [13] Markum H, Pullirsch R and Wettig T 1999 *Phys. Rev. Lett.* **83** 484
- [14] Schindler J, Li A, Zheng M C, Ellis F M and Kottos T 2011 *Phys. Rev. A* **84** 040101(R)
- [15] Li M and Xu T 2015 *Phys. Rev. E* **91** 033202
- [16] Xu T, Lan S, Li M, Li L L and Zhang G W 2019 *Physica D* **390** 47
- [17] Ruschhaupt A, Delgado F and Muga J G 2005 *J. Phys. A* **38** L171
- [18] El-Ganainy R, Makris K G, Christodoulides D N and Musslimani Z H 2007 *Opt. Lett.* **32** 2632
- [19] Makris K G, El-Ganainy R, Christodoulides D N and Musslimani Z H 2008 *Phys. Rev. Lett.* **100** 103904
- [20] Konotop V V, Yang J K and Zezyulin D A 2016 *Rev. Mod. Phys.* **88** 035002
- [21] Suchkov S V, Sukhorukov A A, Huang J, Dmitriev S V, Lee C and Kivshar Y S 2016 *Laser & Photon. Rev.* **10** 177
- [22] Ramezani H, Kottos T, El-Ganainy R and Christodoulides D N 2010 *Phys. Rev. A* **82** 043803
- [23] Sukhorukov A A, Xu Z and Kivshar Y S 2010 *Phys. Rev. A* **82** 043818

- [24] Chen Y J, Snyder A W and Payne D N 1992 *IEEE J. Quantum Electron* **28** 239
- [25] Barashenkov I V 2014 *Phys. Rev. A* **90** 045802
- [26] Pickton J and Susanto H 2013 *Phys. Rev. A* **88** 063840
- [27] Kevrekidis P G, Pelinovsky D E and Tyugin D Y 2013 *J. Phys. A* **46** 365201
- [28] Barashenkov I V, Jackson G S and Flach S 2013 *Phys. Rev. A* **88** 053817
- [29] Moiseyev N and Friedland S 1980 *Phys. Rev. A* **22** 618
- [30] Feng L, Ayache M, Huang J, Xu Y-L, Lu M-H, Chen Y-F, Fainman Y and Scherer A 2011 *Science* **333** 729
- [31] Lin Z, Ramezani H, Eichelkraut T, Kottos T, Cao H and Christodoulides D N 2011 *Phys. Rev. Lett.* **106** 213901
- [32] Regensburger A, Bersch C, Miri M-A, Onishchukov G, Christodoulides D N and Peschel U 2012 *Nature* **488** 167
- [33] Johnson R S 2010 *Singular Perturbation Theory* (New York: Springer-Verlag)
- [34] Li K and Kevrekidis P G 2011 *Phys. Rev. E* **83** 066608